Egyptian Knowledge Bank
https://ijmti.journals.ekb.eg/

International Journal of Materials Technology and Innovation
Volume 3, Issue 2 (2023), pages 10-18

Online ISSN 2682-4299

Effect of GTAW Welding Current on the Quality of 304L Austenitic Stainless Steel Using ER316L

Ahmed Hisham[1,*], Iman El-Mahallawi[1,2], Mohamed R. El-Koussy[2]

[1] The British University in Egypt, Al Shorouk City, Cairo, Egypt
[2] Dept. of Mining, Petroleum and Metallurgical Engineering, Faculty of Engineering, Cairo University, Giza 12613, Egypt.

*Corresponding author: E-mail: Ahmed92020007@bue.edu.eg

Received ……20 February 2023
Accepted ……..9 May 2023
Published……30 June 2023

Abstract

304L is one of the most used stainless steels, usually welded by ER308L but in some cases, welding is performed by ER316L filler according to client specifications or non-nuclear repair. This work focuses on pipes TP304L, with 3mm and 5mm thickness parent metal welded by filler metal ER316L using three welding current levels (75A-105A-135A). The study revealed that no discontinuity in the weld occurred for the three welding current levels and the strength of the weld metal was higher than the base metal. The highest tensile strength for 3mm and 5mm thickness samples was obtained at 105A. The microstructure examination showed that all samples consisted of ferrite and austenite microstructure. The average dendrite length and spacing increased with increasing heat input whereas delta ferrite content decreased with increasing heat input for most of the welded samples. The Microhardness of the welded metal zones for most of the welded samples was lower than the heat-affected zone (HAZ) and parent metal (PM).

Keywords: austenitic stainless-steel, current, gas tungsten arc welding, microstructure, mechanical properties.

1. Introduction

Among the world total stainless-steel production, AISI 300 austenitic stainless-steel covers about 60% of the production. The most used process for welding the AISI 300 stainless-steel group is Gas tungsten arc welding. The process is called (GTAW) or (TIG) and occurs between the non-consumable electrode made from tungsten material and the specimen to be welded by an arc. An inert gas, usually argon, is used to protect the arc from the atmosphere. The selection of proper filler wire and other welding parameters as welding speed, inert gas mixture and joint type are essential factors to achieve optimum mechanical properties, microstructure and quality of the weld shape.

Researchers have investigated process parameters quality of the welded joints correlations. Among all parameters, heat input is the most important because of possible fluctuations during the process. Heat input is a result of voltage, current, speed of welding and section thickness. Reduzan Norizah studied [1] the metallurgical effects due to the variation of current on the 316 Stainless- steels. The study showed that increasing the welding current has a direct impact on the heat-affected zone. The heat affected zone means the weld dimensions (width, and depth of the joint) also the heat input and it is abbreviated as HAZ. At 100A the maximum value of tensile strength was obtained. Weld metal regions showed hardness values less than HAZ and base metal of the welds. Chandra Moi Subhas [2] studied variations of heat inputs on the mechanical and metallurgical properties of GTAW welded joints of SS 316L using ER316L. The study showed that the heat input is directly proportional to the weld bead dimensions, while the height of the weld bead, dendritic and inter-dendritic spacing decreased with the increased values of the heat input. The hardness results showed that the hardness increased from the fusion boundary to the center of the joint. Moreover, the value of hardness for lower heat input condition was higher than higher heat input. The tensile strength of the samples increased up to threshold value and then

decreased with heat input increase. Karthick B studied [3] the mechanical and metallurgical properties of 316 SS joints using 316 SS electrode due to heat input variations. Observations of the tensile test showed that maximum tensile strength was observed at medium heat input followed by low heat input. The value of hardness was high for base metal regions and decreased at the heat affected zone and weld metal. Tandon Vipin studied [4] the microstructural and mechanical characteristics of dissimilar weldments of AISI 316L and AISI 201 using ER316L with different welding currents. Increasing heat input decreases delta ferrite content in the joint. Low heat input (LHI) samples showed higher value of hardness in the fusion zone compared to higher heat input values. The tensile strength for the LHI sample was higher than HHI sample. Chuaiphan [5] studied the mechanical, and microstructural characteristics due to variations of heat input values and gas shielding for SS grade 202 using ER316L. The decrease in heat input increased the ultimate tensile property with smaller dendrite and inter-dendrite spacing sizes. However, longer dendrite size and larger inter-dendrite spacing were observed in the welded joint due to higher heat input in the weld that resulted in reduction of the tensile strength and ductility properties. Ahmed, E studied [6] the impact of heat input and filler wire on AISI 316 using TIG process under different currents. Increasing speed of weld increased the area of the weld, cooling time and solidification time. As heat input increased the UTS, yield strength decreased due to slow cooling rate but grain size of the weld region increased. Lower hardness value at the weld region was observed due to the heat input which causes annealing and recovery while the hardness increases at heat affected zone of the joint from the line of fusion to the sample parent metal due to low rate of cooling which subsequently causes grain growth.

Bahadir [7] studied the mechanical properties of plate AISI 304 using TIG and MIG using three currents with filler 308L. The tensile properties were approximately the same for both processes, but increasing the current level decreased the yield and tensile strength. The hardness profiles for TIG were more uniform compared to MIG. Generally, the hardness increased linearly with increasing current. Tabish T.A. [8] studied the impact of heat input on AISI 304 at three different currents. All welded samples fractured on the parent metal and the highest hardness, and the maximum tensile strength were observed for lower heat input. Kumar et al. [9] studied the mechanical and metallurgical characteristics at different heat inputs of AISI 304 SS joints. The study found that higher heat input affects the mechanical properties of the fusion zone. Moreover, the dendrite length increased. Ogundimu E. O. [10] studied the mechanical and microstructural characteristics of AISI 304 plate due to variation on welding current. It was shown that as the current of welding increased the sample rate of cooling decelerated which permits sufficient time in fusion zone to form dendrites. Moreover, the size of dendrite and spacing of inter-dendrite increased. The strength and ductility were observed higher for the sample with higher current. The hardness shows the same trend for the two samples as there is a slight upturn in hardness values matched with HAZ and base metal. S. A. Rizvi studied [11] the effect of different heat input of plate of 304 austenitic stainless-steel welded using MIG. It was shown that UTS and toughness increased for low heat input. However tensile strength and toughness of the welded samples decreased due to increased heat input. The parent metal (PM) hardness was lower than the heat affected zone of the joints. Higher heat input values decreased the overall value of hardness of weldment. Finer dendrite size was obtained from lower heat input, while larger fusion zone and area was due to higher heat input.

Bansod studied [12] the metallurgical, mechanical characteristics of base metals Cr-Mn SS and AISI 304 joints due to the variation of heat input using SMAW with E308L electrode. Higher values of tensile strength were observed with low heat input samples and due to the effect of increased delta ferrite, improved hardness was observed in the weld zone. Samples with low heat input are associated with fast cooling rate leading to high delta ferrite formation that leads to ferrite formation from the untransformed austenite in FA mode. Nnuka studied [13] the impact of current and type of filler wire on the elongation percentage of AISI304L plate with thickness 3mm welded with filler 308L (Φ 2mm), 309L (Φ 2mm) and 316L (Φ 2.4 mm). It has been observed that the higher current increases the percentage of elongation due to the lower value of thermal conductivity of the base metal which enhances the grain growth with softening effect. The filler ER308L resulted in a higher percentage of elongation for all welding currents due to the lower value of nickel and carbon content. While ER316 showed a constant elongation percentage. Unnikrishnan Rahul studied [14] the impact of current variation on the microstructural property of AISI 304L using SMAW

IJMTI vol. 3, issue2 (2023) 10-18 https://doi.org/ 10.21608/IJMTI.2023.190981.1075

process with filler E308L at three current levels (90-120-160 amperes) for plate thickness 10mm and for plate thickness 6mm with one current level 160 ampere. The penetration, the weld bead width, and fusion area increased with higher values of the heat input. The fusion boundary in the weld region of joints showed skeletal ferrite structure. The dendrite thickness/width was enlarged due to higher values of the heat input. However, the increase in heat input decreased hardness values in the welded region. However, the tensile test was not in the scope of the study.

Most of the research focusing on the impact of welding parameters of ASS304L used ER308 filler; as its common practice however, some industrial situations recommend using ER316L filler grade in repair socket welds, client specification or the availability on the site. 316L has more Ni content in addition to low percentage of (2–3%) molybdenum which results in higher corrosion resistance compared to 304L. Therefore, this work presents an experimental investigation of 304L ASS using ER316L filler to evaluate the mechanical and microstructure performance of welds at three different currents (75A-105A-135A). All three investigated currents are within the range of recommended industrial practice.

2. Experimental Work

In this research austenitic stainless-steel pipe TP304L with outside diameter 75mm and two different thicknesses 3mm and 5mm was used as the workpiece. The single V welds with bevel angle 37.5º ±2.5 and face root about 0.8mm with root gap 1.2mm were prepared by cutting using power saw. Moreover, the samples were turned on the lathe machine.

The chemical compositions of parent metal 304L and ER316L filler wire used are shown in Table 1 according to the material test certificate. The low percentage of carbon is used to decrease the intergranular corrosion possibility whereas the 2-3% percentage of molybdenum enhances the resistance of pitting corrosion property of the weldment. In addition the small percentage of molybdenum as 0.5 wt% increases the tensile strength of austenitic stainless-steel in elevated temperature.

Molybdenum is an element that promotes the ferrite phase formation and retention in the microstructure. However austenitic stainless-steel contains higher level of nickel content to establish and promote the formation of austenitic phase while chromium content is responsible for the ferrite microstructure formation and retention. Balancing between ferrite and austenitic promotion elements controls the metallurgy, mechanical properties and weldability of stainless-steel [15].

Table1 Chemical composition of the parent metal 304L and filler ER316L

Chemical Composition (wt.%)		
Elements	B.M(304L)	Filler(316L)
C	0.024	0.025
Ni	10.18	11.25
Mn	0.89	1.73
P	0.031	0.027
Si	0.44	0.35
S	0.03	0.012
Cr	16.29	19.30
Mo	2.04	2.26
Cu		0.38

The GTAW process was conducted using HUGONGPOWER TIG 300DPIII machine by a qualified and certified welder and the WPS was prepared and followed. Butt joint configurations were used for all samples. The GTAW welding process used three different current levels (75-105-135) A. The pipes were tacked and fixed on the welding table with L angle for the fixture as shown below in Fig.1.

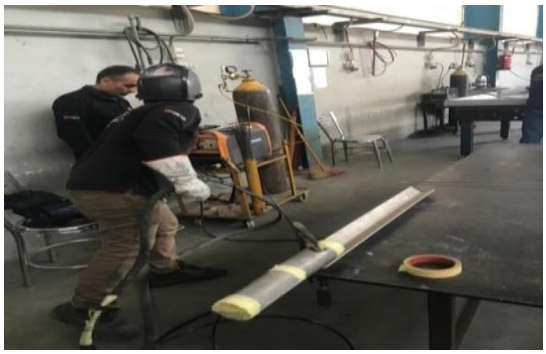

Fig. 1 Pipe fixation

The parameters of the GTAW process are shown in Table 2.

Table 2 Welding Parameters of GTAW

Tungsten electrode diameter	2.4mm
Filler rod diameter	1.6mm
Welding current	75A,105A and 135A
Shielding gas	Argon 5-7L/min
Purge gas	Argon 10L/min
Gas purity	99.9%

IJMTI vol. 3, issue2 (2023) 10-18 https://doi.org/ 10.21608/IJMTI.2023.190981.1075

The welding current parameter is considered a dominant factor that has direct impact on mechanical and microstructure of the joint, in addition to its direct impact on the heat input and melting rate of the filler rod. Hence, welding was performed at three different levels of currents (75-105-135) for 3mm and 5mm thicknesses. Calculation of heat input was done according to Equation (1).

$$\text{Heat input } \left(\frac{\text{kJ}}{\text{mm}}\right) = \frac{\text{I} \times \text{V}}{\text{S} \times 1000} \quad (1)[12]$$

The heat input per layer and total heat input at different levels for welded samples are shown in Table 3 I is initially the current of welding in ampere (A), S is the welding speed in mm/s and finally the arc voltage is V in volt (V). After completion of welding joints, the joints were inspected by visual and phased array ultrasonic testing (PAUT) to examine the soundness of the welded samples. Although the recommended thickness for ASME, BS and EN standards is 6mm and over, the PAUT technique is used in field site as common practice from thickness 3mm and over for demonstrating artificial defects during calibration [16]. It is observed from the study [16] that PAUT provides high detection for welds of material with 4 and 5mm thickness where flaws are clearly identified from the results. Moreover, a study [17] shows that the PAUT inspection of thin stainless-steel welds of 3.25mm thickness using TIG process has the capability of detecting 0.35mm mean defect with a confidence level higher than 98%. Samples for tensile test were cut perpendicular relative to the direction of welding and the tensile test was performed on the joints by using hydraulic universal testing machine SHIMADZU (UH-600kNX C1). Dog-Bone shape welded samples were prepared and machined with milling machine and according to ASME IX Ed.2021 with dimensions in figure QW-462.1(b). The tensile samples were cut in the perpendicular direction of the joint and the weld joint was ensured to be in the center of the specimen gauge length.

The samples were cut from the welded samples using angle grinder tool, for microstructure characterization, in transverse sections of the welded samples. Grinding was carried out for the joints using grinding and polishing wheel machine. The grinding process used coarser Silicon Carbide sandpapers P320, P600, P800, P1200 and P2000 for about 3min for each sand paper with water as lubricant. Polishing was performed using aluminium oxide with average grain size 0.5µm. The welded samples were etched using electrolytic oxalic acid etchant consisted of 10 g of ($C_2H_2O_4$) oxalic acid and 100 mL distilled water at 6 Volt for 1 minute as per ASTM E407-07 edition 2012 standard. An optical microscope (Olympus BX41M-LED) equipped with image-analyzing software was used to examine the microstructural properties of the joints. The analysis of delta ferrite content on the weld metal was performed using a Ferritescope (Fischerscope) Model FMP30. Different sample points were measured and the average value was obtained.
The hardness test was performed using (Zwick/Roell) ZHU 250 machine according to Vickers hardness scale. The hardness test was performed using an indenter of diamond material with 10 kg load and a lens 185x for magnification with field view diameter of approximately 0.8 mm at room temperature. The measurements were made at the parent metal, heat-affected zone, and fusion zone of the joint respectively with three measurements.

Table 3 Heat input calculation for welded sample

Sample	Volt	Time	Average for total heat input
644 (3mm)/75A	11:12.6	4.25	1.71:1.95
	12.4:14	3.48	
647 (5mm)/75A	10.8:12	8:30	5.12:5.83
	9.8:11.6	5:15	
	10.5:11.8	5:39	
	9.8:11.5	3:78	
	9.7:10.8	3:58	
645 (3mm)/105A	11.6:13.4	2:54	1.53:1.7
	13.5:14.4	2:05	
648 (5mm)/105A	10.5:11.7	6:35	4.86:5.4
	9.5:10.8	4:13	
	9.8:10.8	5:35	
	11.5:12.5	2	
646 (3mm)/135A	11:14	4:07	2.58:3.11
	14:15.5	2:15	
649 (5mm)/135A	11:14	5:50	5.04:5.97
	10:12	2:53	
	10:12	2:40	
	10.5:11.5	3:50	

3. Results and Discussion

3.1 Metallography

3.1.1 Macrostructure

The macrostructure of sample no.648 weld metal is shown below in Figure 2. The weld dimensions as the width of the face and root, in addition to the average

length of the dendrite and average spacing of dendrite joints, are shown Table 4. It's shown that with the incremental increase in heat input, the face and root of the welded samples width increased.

Fig. 2 Macrostructure of sample no.648 weld metal

Table 4 Weld dimensions of welded samples

Specimen	Width of face weld (mm)	Width of the root weld (mm)	Average Dendrite length (µm)	Average Dendrite spacing (µm)
644	8.7	7	4.103	17.73
645	8.3	6.5	2.73	16.24
646	8.9	7.2	5.8	22.298
647	16	7.5	3.7	16.923
648	12.6	6.8	2.59	12.3
649	14	7.3	3.2	15.78

3.1.2 Microstructure

The microstructure of the parent metal of AISI304L and the welded specimen are shown below (in Figs. 3, 4, and 5) which were observed using an optical microscope (Olympus BX41M-LED). The microstructure study shows that the parent metal is austenite as shown in Figure 3. Moreover, fusion zone (FZ) of the joints at different current levels consists of austenite phase (bright spots) and ferrite phase (dark spots). An example of FZ welded samples at different currents is shown below in Figures 4 and 5. The ferrite content acts as a strengthening agent in the welded joints leading to an increase in the tensile strength of the weld relative to the parent metal [15].

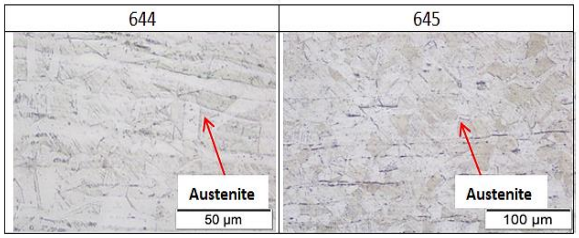

Fig. 3 Microstructure of the parent metal

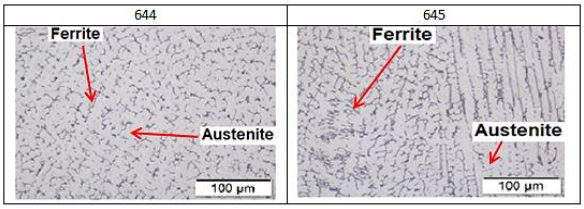

Fig. 4 Microstructure of the welded samples

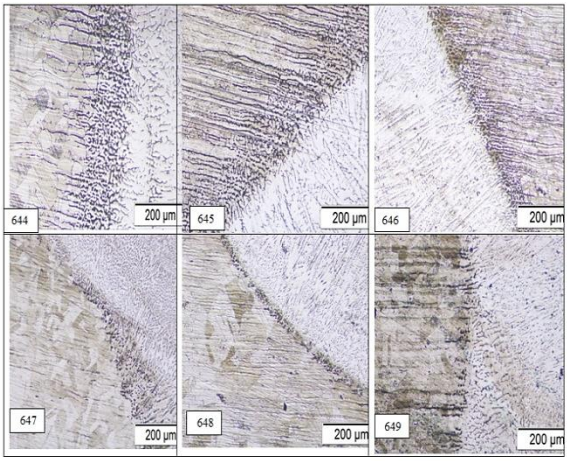

Fig. 5 Microstructure of welded samples showing HAZ and parent metal

The average length of dendrite and average spacing of dendrite values at different current levels are shown in Table 4 where the average length of dendrite and average spacing of dendrite increase with increasing heat input. As higher values of heat input gives sufficient time for dendrite structure to widen in the weld zone which agrees with literature [9, 10]. It is observed from the Equation (2) that the heat input is inversely proportional to the rate of cooling [18].

$$R = \frac{2\pi k(T_c - T_o)^2}{H_{net}} \quad (2)$$

Where R= the rate of cooling at center line of the weld °C/s
k=thermal conductivity of the metal J/mm.s °C
Tc= 550 °C (Constant for most steels)
To= Room temperature
Hnet= Heat input
The increase in dendrite structure length due to the low rate of cooling is related to high heat input which allows grain growth in sufficient time. In addition to the width of PMZ, HAZ grain increased in agreement with literature [1, 14, 18].

IJMTI vol. 3, issue2 (2023) 10-18 https://doi.org/ 10.21608/IJMTI.2023.190981.1075

3.1.3 Solidification mode

The Constitution Diagram of stainless-steel weldments (WRC-1992) for the present work is shown in Figure 6 and was used to calculate the ferrite percentage content relative to the Chromium (Creq) and Nickel (Nieq) equivalents of the welded samples according to equations (3) and (4)[19].

$$Creq=Cr+Mo+0.7Nb \quad (3)$$

$$Nieq=Ni+35C+20N+0.25Cu \quad (4)$$

The Chromium, Nickel equivalents (Creq),(Nieq) respectively are shown in Table 5. The chemical composition is determined according to the Material Test Certificate (MTC) and reviewed according to specification SA312 in ASME II part A Edition 2021.

Table 5 Chemical composition, Creq /Nieq

Chemical Composition (wt.%)		
Elements	B.M(304L)	Filler(316L)
C	0.024	0.025
Ni	10.18	11.25
Mn	0.89	1.73
P	0.031	0.027
Si	0.44	0.35
S	0.03	0.012
Cr	16.29	19.30
Mo	2.04	2.26
Cr_{eq}	18.33	21.56
Ni_{eq}	11.02	12.125
Cr_{eq}/Ni_{eq}	1.66	1.77

Austenite mode of the weld pool: L → (L + ɣ) → ɣ; where Creq⁄Nieq < 1.25

Austenite −Ferrite (AF)mode: L → (L + ɣ) → (L + ɣ + δ) → (ɣ + δ); 1.25 < Creq⁄Nieq < 1.48

Ferrite − Austenite (FA)mode : L → (L + δ) → (L + δ + ɣ) → (ɣ + δ); 1.48 < Creq⁄Nieq < 1.95

Ferrite(F) mode: L → (L + δ) → δ → (ɣ +δ); Creq⁄Nieq > 1.95

3.1.4 Ferrite Number Measurements

The delta ferrite content in the fusion zone was observed in terms of average readings of ferrite number measured using ferrite scope as shown below in Table 6. It can be observed that for most of the welded samples the delta ferrite content decreases with increasing heat input. Where the rate of cooling is relatively high for lower heat input as shown in equation (2) that results in lower time for the transformation of delta ferrite to austenite phase. While for high heat input associated with lower rate of cooling there is a sufficient transformation time from delta ferrite to austenite phase this agrees with Vipin [4].

It is observed that the overall delta ferrite for samples with 3mm thickness is higher than samples with 5mm thickness due to the lower cooling rates associated with higher thickness. From the WRC-1992 diagram it is observed that the mode of solidification of the joints is ferrite-austenite (FA) mode which minimizes solidification cracks occurrence.

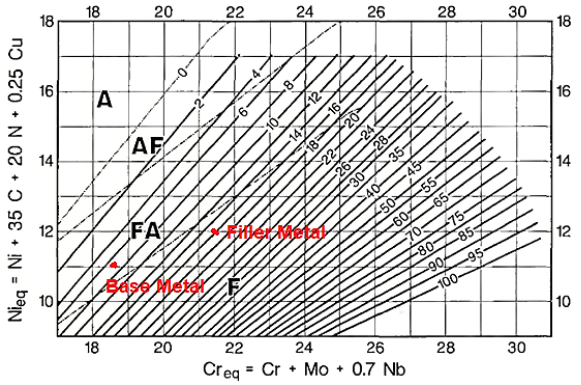

Fig. 6 WRC-1992 diagram for solidification mode of welded samples [19].

Table 6 Ferrite Number measurements.

Sample No	FN Number in Weld metal
644	5.65±1.55
645	7.5±1.7
646	7.2±1.4
647	5.9±0.8
648	6.85±1.25
649	.62±0.8

3.2 Phased Array Ultrasonic Testing

Phased array ultrasonic testing (PAUT) records are shown in Figure 7 of the welded samples, demonstrating that the weldments are sound with full penetration and free from the weld discontinuities such as porosity, slag, incomplete of penetration and incomplete of fusion. Therefore, the welding parameters applied during welding are appropriate.

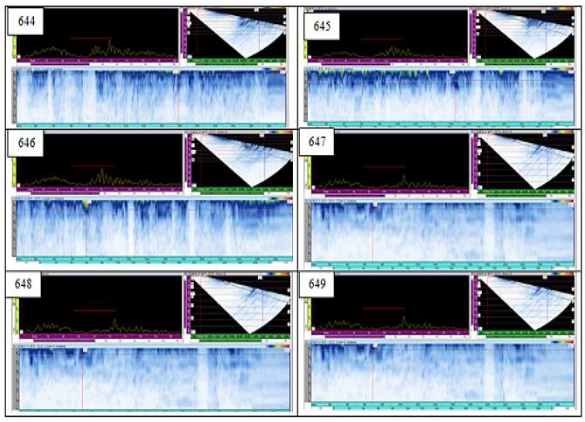

Fig. 7 PAUT for welded samples

3.3 Hardness test

The hardness values for parent metal, weld metal and heat affected zone (HAZ) for joints are shown in Table 7. It is shown that the hardness for the heat-affected zone and the parent metal (for most of welded samples) are higher than those of the weld metal [3], due to microstructure changes and the impact of delta ferrite phase forming in the welded metal zone. Generally, the hardness value of the austenitic phase is higher compared to delta ferrite phase [5]. Lower hardness values observed in the weld metal are due to the heat generated from the process of welding which causes annealing and recovery. Where the HAZ shows higher hardness values due to the low rate of cooling which subsequently causes grain growth which agrees with the literature [6, 12, 14, 18]. However the hardness of sample 645 on heat affected zone (HAZ) is lower than the weld zone due to the fast rate of cooling which results in a microstructure with less average values of dendrite spacing that agrees with literature [8, 11].

3.4 Tension test

The ultimate tensile strength of the welded samples is shown below in Figure 8. In this work, the strength of the joints decreased with heat input as the highest strength was obtained for lowest heat input for both 3 and 5 mm thick pipes. However, it has been reported in previous work that the strength increases till a threshold value and then starts to decrease as Subhas [2].

All joints fractured at the parent metal as the welded samples strength is higher than the parent metal. Lower heat input welded samples exhibit higher tensile strength. As increasing heat input; softens and coarsens the grains forming due to the lower rate of cooling in addition to the tensile strength decrease. In addition to, the lower values of heat input result in increased content of delta ferrite on the fusion zone as the strength of the weld increase due to fast rate of cooling.

Table 7 hardness value for the parent metal, weld metal and HAZ respectively

S. No	Hardness								
	Parent Metal			Weld Metal			HAZ		
644	220	212	198	184	177	172	207	193	202
645	234	220	231	262	257	277	239	247	242
646	232	240	244	222	224	229	232	236	243
647	227	235	243	233	245	234	241	247	245
648	238	242	244	233	221	238	243	248	246
649	211	218	209	244	239	236	221	220	209

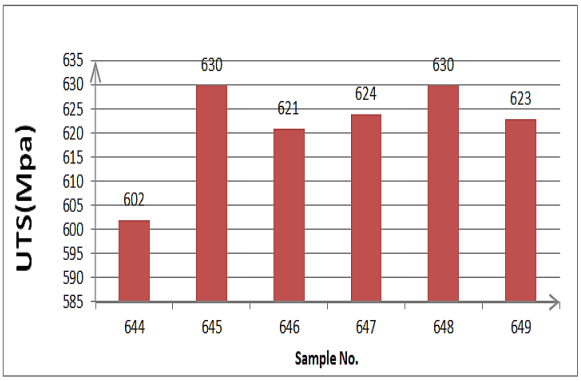

Fig. 8 UTS for welded samples

The tensile strength property of all welded samples decreases with increasing heat input this agrees with Vipin [4]. This is due to the slow rate of cooling associated with higher input of heat which leads to an increase of the grain size on the weld region [18]. High heat input results in microstructures with long average dendritic sizes and average dendritic spacing in the weld leading to reduced tensile strength which agrees with literature [5]. The UTS of joints in the study is higher than joints of 316 Parent metal welded with ER316L where maximum tensile strength 560 MPa is observed with low heat input at current 80A [6]. However, in the case of welding of AISI 304 with ER308L UTS was 641 MPa at the current of 90A while 470MPa was obtained at a Current of 110A [7]. This suggests that using filler ER316L reduces fluctuations in the strength results with changes in current within the common practice recommended range

This study has focused on a commonly used group of steels in many industrial sectors. Despite the fact that the welding technologies for stainless-steels have matured and data and process sheets are available by

many welding services providers, new challenges appear daily due to new challenging requirements of failures and changes in the service environment that leads to incompatibility of the stated facts regarding the filler metals and process parameters limitations. As stated earlier in the introduction, the studied alloy ASS304L is designated in most process sheets of welders to be welded with ER308 filler. However, using ER316L offers advances in the service conditions when corrosion of the welded joints is a challenge. According to field observations and research efforts, fluctuations in heat input also present a challenge due to its effect on the HAZ. This work shows that using ER316L combined with current levels in the range identified by standard industrial codes fulfill industrial requirements.

4. Conclusions

The conclusions of this work are a result of experimental work on welding of AISI 304L with ER316L performed by GTAW process at different welding currents (75-105-135) ampere.

The following conclusions were observed from the current investigation.

1. Using current in the range 75-135A resulted in sound weld with no defects and the joints were free of porosity, cracks, lack of fusion or lack of penetration.
2. The microstructures consisted of austenite and delta ferrite for the different current levels. The average dendrite length and spacing increases with increasing heat input. As lower heat input promotes higher tensile strength while higher heat input resulted in reduced tensile strength.
3. The weld metal solidification mode was FA mode without solidification cracks. This means that delta ferrite content is appropriate for avoiding solidification cracking.
4. The width and the face and root of the joint increase with increasing heat input.
5. The delta ferrite content decreases with increasing heat input for most of the welded samples
6. The microhardness of the welded metal zones for most of the welded samples was lower than the heat-affected zone (HAZ) and parent metal (PM).
7. All joints fractured at the parent metal which indicates that the welded specimen strength is higher than the parent metal.

References

[1] Redzuan ,N.; Moslemi ,N.; Ahmad N.; Nan Hor,. “Effect of current on characteristic for 316 stainless steel welded joint including microstructure and mechanical properties” 12th Global Conference on Sustainable Manufacturing.

[2] Chandra ,M,S.; Pal, K, P.; Bandyopadhyay,A.; Rudrapat,R. “Effect of Heat Input on the Mechanical and Metallurgical Characteristics of TIG Welded Joints” Journal of Mechanical Engineering Vol 16(2), 29-40, 2019.

[3] Karthick,B.;Shrihari,L.:Sakthivel,M.:Shriram,S. ;Silambarasan,V.“Effect of Heat Input on the Microstructure and Mechanical Properties of Gas Tungsten Arc Welded AISI 316 Stainless Steel Joints” INTERNATIONAL RESEARCH JOURNAL ON ADVANCED SCIENCE HUB Vol.02 No.08 August 2020.

[4] Tandon,V .;Manish,A. T.;Awanikumar, P, P.;Ravindra V, T.; Himanshu,V.; “Eff¬ect of heat input on the microstructural, mechanical, and corrosion properties of dissimilar weldment of conventional austenitic stainless steel and low nickel stainless steel” Metallography, Microstructure and Analysis (2020) 9:668–677.

[5] Chuaiphan, W.; Srijaroenpramong, L. “Heat input and shielding gas effects on the, microstructure mechanical properties and pitting corrosion of alternative low cost stainless steel grade 202” Results in Materials Vol.7 ,2020.

[6] Ahmed,E.;Ahmed,R.; EL-Nikhaily,A.; Essa,A.R.S.; “Effect of heat input and filler metals on weld strength of gas tungsten arc welding of AISI 316 weldments” CHINA WELDING Vol. 29 No. 1 .

[7] Iscan, B.; Onar,V.; Ulkoy,A. “Investigation of the mechanical properties of AISI 304 austenitic stainless steel joints produced by TIG and MIG welding methods using 308L filler wire” International Journal of Innovative Research in Science, Engineering and Technology Vol. 6, Special Issue 10, May 2017.

[8] Tabish,T.A.;Abbas,T.;Farhan ,M.; Atiq.S.; Butt,T,Z. “Effect of heat input on microstructure and mechanical properties of the TIG welded joints of AISI 304 stainless steel” International Journal of Scientific & Engineering Research, Vol.5, no. 7, July-2014.

[9] Kumar, S.; Shahi, A. “Effect of heat input on the microstructure and mechanical properties of gas tungsten arc welded AISI 304 stainless steel joints” Materials & Design ,Vol. 32, no.6, pp. 3617-3623.

[10] Ogundimu ,E. O.; Akinlabi ,E. T.; Erinosho,M. “Effect of Welding Current on Mechanical Properties and Microstructure of TIG Welding of Type-304 Austenite Stainless Steel”

International Conference on Engineering for Sustainable World (2019).
[11] Rizvi, S. A. "Effect of Heat Input on Microstructural and Mechanical Properties of AISI 304 Welded Joint Via MIG Welding" International Journal of Engineering Vol. 33, No. 9, pp. 1811-1816.Zhang H., ACS Nano (2015). doi. org/10.1021/acsnano. 5b05040.
[12] Bansod, A.V.; Patil, A.P.; Moon, A.; Shukla, S. "Microstructural and Electrochemical Evaluation of Fusion Welded Low-Nickel and 304 SS at Different Heat Input"2017, 26, 5847–5863.
[13] Nnuka, E. E., Okonji P. O. "Effect of welding current and filler metal types on percent elongation of GTAW austenitic stainless steel weld joints" European Journal of Material Sciences Vol.2, No.1, pp.26-31.
[14] Unnikrishnan,R.;Satish Idury,K.S.N.;Ismail,T.P.;Bhadauria.A.;Shekha wat.S.K.;Rajesh.K.K.; Sanjay,G,S.; "Effect of heat input on the microstructure, residual stresses and corrosion resistance of 304L austenitic stainless steel weldments" Materials Characterization, Vol. 93, pp. 10-23.
[15] Lippold.C.J & Kotecki.J.D. "Welding Metallurgy and Weldability of Stainless steels, (2005).
[16] Carpentier.C and Rudlin.J "Manual ultrasonic inspection of thin metal welds 11th European Conference on Non-Destructive Testing (ECNDT 2014) " 2014.
[17] Pettigrew, I., Bird, C., & Bell, D. (2013). "A Phased Array Inspection Solution for the Assessment of Thin Stainless Welds"9th International Conference on NDE in Relation to Structural Integrity for Nuclear and Pressurized Components(2012)
[18] Welding Handbook Seventh Edition, "Volume 1 Fundamentals of Welding, AWS, American Welding Society, 1976.
[19] Kotecki, D.; Siewert, T. "WRC-1992 Constitution Diagram for Stainless Steel Weld Metals"Weld. J. 1992, 71, 174.